Published in final edited form as:
Cell. 2013 February 14; 152(4): 778–790. doi:10.1016/j.cell.2013.01.023.

mTor Regulates Lysosomal ATP-sensitive Two-Pore Na^+ Channel to Adapt to Metabolic State

Chunlei Cang[#1], **Yandong Zhou**[#1], **Betsy Navarro**[2], **Young-jun Seo**[1], **Kimberly Aranda**[1], **Lucy Shi**[1], **Shyuefang Battaglia-Hsu**[3], **Itzhak Nissim**[4], **David E. Clapham**[2], and **Dejian Ren**[1,†]

[1] Department of Biology, University of Pennsylvania, 415 S. University Ave., Philadelphia, Pennsylvania 19104, USA

[2] Howard Hughes Medical Institute, Department of Cardiology, Children's Hospital, Boston, Massachusetts 02115, USA

[3] INSERM U954, Nutrition Génétique et exposition aux risques environnementaux Faculté de Médecine - BP 184, Université de Lorraine, 54505 VANDOEUVRE LES NANCY CEDEX, FRANCE

[4] Division of Child Development and Metabolic Disease, Children's Hospital of Philadelphia, Department of Pediatrics, Biochemistry and Biophysics, University of Pennsylvania School of Medicine, Philadelphia, PA 19104, USA

[#] These authors contributed equally to this work.

SUMMARY

Survival in the wild requires organismal adaptations to the availability of nutrients. Endosomes and lysosomes are key intracellular organelles that couple nutrition and metabolic status to cellular responses, but how they detect cytosolic ATP levels is not well understood. Here we identify an endolysosomal ATP-sensitive Na^+ channel ($lysoNa_{ATP}$). The channel is a complex formed by Two-Pore Channels (TPC1 and TPC2), ion channels previously thought to be gated by nicotinic acid adenine dinucleotide phosphate (NAADP), and the mammalian target of rapamycin (mTOR). The channel complex detects nutrient status, becomes constitutively open upon nutrient removal and mTOR translocation off the lysosomal membrane, and controls the lysosome's membrane potential, pH stability, and the amino acid homeostasis. Mutant mice lacking $lysoNa_{ATP}$ have much reduced exercise endurance after fasting. Thus, TPCs are a new ion channel family that couple the cell's metabolic state to endolysosomal function and are crucial for physical endurance during food restriction.

[†]***To whom correspondence should be addressed:***dren@sas.upenn.edu Phone: (215) 898-9271 Fax: (215) 898-8780.

Author Contributions

CC designed experiments and contributed all the patch clamp recordings. YZ did protein chemistry experiments, immunocytochemistry and lysosomal pH imaging. YS performed protein chemistry and ATP measurements. YS and IN did amino acid analysis. CC and YZ performed amino acid efflux assay. DR initiated the project, designed experiments, developed cDNA constructs and the mouse models, and performed the behavior studies. BN and SBS performed pilot studies. KA and LS developed reagents. DR and DEC supervised the projects. CC, DEC, and DR wrote the manuscript.

SUPPLEMENTAL INFORMATION

Supplemental Information includes extended experimental procedures, supplemental references and 5 supplemental figures.

INTRODUCTION

Cells use adenosine triphosphate (ATP) as an energy carrier. Sensing intracellular concentrations of ATP ([ATP]) is a crucial step in the regulation and coupling of [ATP] to cellular metabolism. One of the most extensively characterized cellular ATP sensors is the plasma membrane ATP-sensitive K^+ channel (K_{ATP}) (McTaggart et al., 2010; Nichols, 2006; Noma, 1983). K_{ATP} channels are important for coupling between glucose concentration and insulin secretion in pancreatic β cells, the protection of the heart during stress and the coupling of [ATP] to neuronal excitability (McTaggart et al., 2010; Nichols, 2006, for review). In contrast to channels on the plasma membrane that regulate such functions as secretion, intracellular ion channels are more difficult to study and thus are less well understood. For example, ATP-sensitive K^+ channels (mitoK_{ATP}) have been recorded from the mitochondrial inner membrane (Inoue et al., 1991), but their molecular identities are not established (Foster et al., 2008). Although it is clear that endosomes and lysosomes play key roles in cellular metabolism, we do not understand how metabolic signals are received by these organelles. Here we report an ATP-sensitive Na^+ channel (lysoNa$_{ATP}$) on endolysosomal membranes that is responsive to physiological [ATP]. The channel is formed by TPC1 and TPC2, two well-conserved proteins whose functions are largely unknown. The channel associates with the mammalian target of rapamycin (mTOR) complex and detects cellular nutrient status, becoming constitutively open when nutrients are depleted and when mTOR translocates away from the complex at the lysosomal membrane. LysoNa$_{ATP}$ determines the sensitivity of endolysosome's resting membrane potential to Na^+ and cytosolic ATP, controls lysosomal pH stability and regulates whole-body amino acid homeostasis. Strikingly, mutant mice lacking *tpc1* and *tpc2* have severely reduced endurance after fasting.

RESULTS

Endolysosomes Have a Novel ATP-sensitive Na^+-permeable Channel lysoNa$_{ATP}$

To determine whether endolysosomes have ionic mechanisms that sense intracellular physiological [ATP], we recorded whole-endolysosomal currents from endosomes/lysosomes mechanically released from the cytosol with a glass pipette (Saito et al., 2007). Endolysosomes were enlarged by treatment of cells with vacuolin-1, as previously described (Cerny et al., 2004; Dong et al., 2008). The optimal activities of many plasma membrane channels require phosphatidylinositol 4,5-bisphosphate ($PI(4,5)P_2$) as a co-factor to prevent channel “run-down” (Hilgemann et al., 2001; Suh and Hille, 2008; Wu et al., 2002). Similarly, $PI(3,5)P_2$, a phosphatidylinositol bisphosphate primarily found in intracellular organelle membranes, increases channel currents in endolysosomes (Dong et al., 2010). We first recorded endolysosomal currents from mouse peritoneal macrophages, where lysosomes are well studied. Little current was detected when pipette solution contained 150 mM K^+ but no Na^+ (−5.6 ± 2.3 pA with no $PI(3,5)P_2$ in the bath and −7.7 ± 2.1 pA with 1 μM $PI(3,5)P_2$; n = 7, −100 mV). With a pipette solution containing Na^+ (a major cation in the endolysosomal lumen (Steinberg et al., 2010)) and K^+ in the cytosolic solution containing $PI(3,5)P_2$, we recorded large inward currents (Na^+ moving out of the endolysosome into the cytosol, Figure 1A) when no ATP was present in the bath (Figure 1B, C). Upon addition of ATP-Mg, however, the amplitude of the Na^+ current was reduced in a dose-dependent manner with an IC_{50} of 0.32 ± 0.05 mM and a Hill coefficient of 1.25 ± 0.20 (Figure 1B-E). Thus, peritoneal macrophage endolysosomes have an ATP-sensitive Na^+-permeable channel (lysoNa$_{ATP}$) sensitive to physiological [ATP]. Similar lysoNa$_{ATP}$ currents were also detected in endolysosomes from other cell types we tested, including excitable cells such as beating cardiac myocytes and nonexcitable cells such as fibroblasts and liver hepatocytes (Figure 1F-K).

TPCs Form lysoNa$_{ATP}$ Channels in HEK293T Cells

We used a candidate approach to identify proteins that reconstitute lysoNa$_{ATP}$ when transfected into HEK293T cells (these cells have little endogenous lysoNa$_{ATP}$; Figure 2A). Among the hundreds of known ion channels, TRPML1 (a 6-transmembrane spanning endolysosomal Na^+-permeable cation channel in the TRP family) and TPC1/TPC2 proteins (endolysosomal channels of 12-transmembrane spanning proteins with similarity to that of voltage-gated Na^+ and Ca^{2+} channels) are known to localize on endosomes and lysosomes (Brailoiu et al., 2009; Calcraft et al., 2009; Grimm et al., 2012; Ishibashi et al., 2000; Pryor et al., 2006). We recorded endolysosomal currents from HEK293T cells transfected with candidate proteins tagged with GFP. I_{TRPML}, though potentiated by exogenously applied $PI(3,5)P_2$ (Dong et al., 2010), was not sensitive to ATP, either at saturating concentrations (1 μM) (Figure 2B, Figure S1A) or a concentration close to its EC_{50} (0.1 μM) (Figure S1B).

Strikingly, overexpression of human TPC1 increased endolysosomal ATP-sensitive currents by 13-fold (Figure 2C). Similarly, transfection with TPC2 resulted in a large lysoNa$_{ATP}$ current (Figure 2D, E) sensitive to [ATP] (IC_{50}= 0.92 ± 0.31 mM; Figure 2D), comparable to that recorded from macrophages. Since TPC2 has more prominent lysosomal localization than TPC1 (Calcraft et al., 2009) and is more readily identified in patch clamp recordings, we focused on TPC2. In controls, GFP-tagged and -untagged TPC2 generated similar lysoNa$_{ATP}$ currents (Figure S1C). ATP's inhibition of lysoNa$_{ATP}$ was not mediated by changes in free calcium ([Ca^{2+}]=117 nM without ATP and 118 nM with 1 mM ATP). Application of ATP-Mg also increased the free Mg^{2+} concentration (1.94, 1.99, and 2.18 mM in the presence of 0, 1 and 5 mM ATP-Mg, respectively), but lysoNa$_{ATP}$ was not sensitive to Mg^{2+}, as addition of Mg^{2+} alone did not affect current amplitudes (Figure S1D). Unlike K_{ATP} (Nichols, 2006), lysoNa$_{ATP}$ is insensitive to ADP (Figure 2E). Similarly, GTP did not inhibit lysoNa$_{ATP}$ (Fig. 2F). In summary, ~ 0.9 mM [ATP], a level found in nutritionally replete cells, inhibits the TPC-mediated endolysosomal Na^+ current and this inhibition is mediated directly by ATP or ATP-Mg.

The ATP-sensitivity of plasma membrane K_{ATP} can be drastically shifted from several μM toward physiological mM concentrations by the plasma membrane species of PIP_2, $PI(4,5)P_2$, as a result of interaction between the phospholipid and the channel gating machinery (Baukrowitz et al., 1998; Shyng and Nichols, 1998). Organellar PIP_2 ($PI(3,5)P_2$), however, had no major effect on lysoNa$_{ATP}$'s ATP sensitivity (Figure 2D). In addition, basal I_{TPC2} was readily recorded from endolysosomes without the addition of $PI(3,5)P_2$ in TPC2-transfected cells and the currents were also inhibited by ATP (Figure S1E). Therefore, the ATP sensitivity of the lysoNa$_{ATP}$ channels is independent of $PI(3,5)P_2$.

Although TPC channels had been proposed to be activated by nicotinic acid adenine dinucleotide phosphate (NAADP) (Calcraft et al., 2009), recent data suggest that TPC proteins are not the direct targets of NAADP (Lin-Moshier et al., 2012; Wang et al., 2012). One potential mechanism for NAADP activation could be the release of ATP inhibition of TPC channels. However, NAADP had no effect on the ATP inhibition of lysoNa$_{ATP}$ recorded from macrophages (Figure S1F) or TPC2-transfected HEK293T cells (Figure S1G), suggesting that NAADP is not an activator of TPCs in the lysoNa$_{ATP}$ complex.

lysoNa$_{ATP}$'s ATP Sensitivity Requires mTOR

Unlike the plasma membrane K_{ATP} channel, which is inhibited by both ATP and the nonhydrolyzable analog ATPγS by direct binding (Nichols, 2006), lysoNa$_{ATP}$ is not inhibited by ATPγS (Figure S1H). Interestingly, the inhibition of lysoNa$_{ATP}$ by ATP is slow ($T_{1/2}$: 43.3 ± 8.8 s, n = 3, Figure S1I), in contrast to the fast inhibition of K_{ATP} (ms). These slow kinetics were not due to ATP diffusion from cytosol (bath) to the lumen since dialyzing

the endolysosomal lumen with 10 mM ATP in the pipette solution did not block lysoNa$_{ATP}$ and the channel was still inhibited by ATP applied in the bath (Figure 2G). We conclude that ATP acts on the channel from the cytosolic surface of the endolysosome. The slow kinetics and the requirement of ATP hydrolysis suggest that ATP does not directly bind TPC to inactivate it. We next examined whether a slower process, such as activation of protein kinases, is responsible for lysoNa$_{ATP}$'s ATP sensitivity.

A well-established cytosolic ATP-sensing kinase is the AMP-activated protein kinase (AMPK) (Hardie et al., 2012; Oakhill et al., 2012). In the presence of an AMPK inhibitor dorsomorphin, however, lysoNa$_{ATP}$ was still ATP-sensitive (Figure S2A). In addition, lysoNa$_{ATP}$ recorded from TPC2-transfected MEF cells lacking both AMPK catalytic subunit isoforms (AMPK 1/2 double knockout, dKO) was readily inhibited by ATP (Figure S2B). Thus, lyosNa$_{ATP}$'s ATP sensitivity does not require AMPK.

Under our recording configurations where soluble proteins are easily washed away (Figure 1A), a putative functional kinase should be associated with the endolysosomal membrane and TPC. One of the few kinases known to be tethered to the lysosome membrane is the mammalian target of rapamycin (mTOR) (Korolchuk et al., 2011; Sancak et al., 2010; Zoncu et al., 2011). Consistent with the role of mTOR in lysoNa$_{ATP}$'s ATP sensitivity, the mTOR inhibitors rapamycin and Torin 1 profoundly reduced the ATP sensitivity of reconstituted lysoNa$_{ATP}$ in TPC2-transfected HEK293T cells (Figure 3A-C) and that of the native channel in macrophages (Figure 3D-F, Figure S2C).

To test whether the ubiquitously expressed mTOR protein is required for lysoNa$_{ATP}$'s ATP sensitivity, we knocked down the endogenous mTOR protein in HEK293T cells using lentivirus encoding an shRNA against human mTOR (Figure 3G). The ATP sensitivity of lysoNa$_{ATP}$ generated by TPC2 in the mTOR shRNA virus-infected cells was dramatically lowered to ~ 5 mM (Figure 3I, J). A control, scrambled shRNA had no significant effect (Figure 3H, J).

Two mTOR complexes are active in mammalian cells ((Laplante and Sabatini, 2012a) for review), the Raptor-containing mTORC1 and Rictor-containing mTORC2. Knockdown of Raptor (Figure 3L), but not Rictor (Figure 3K), reduced the ATP inhibition of the channel (Figure 3M), suggesting that lysoNa$_{ATP}$'s ATP sensitivity is conferred by mTORC1.

TPC Complexes with mTOR

mTOR was co-immunoprecipitated with TPC1 or TPC2 from transfected HEK293T cells (Figure 4A), suggesting that the channel proteins and mTOR are in the same signaling complex. We did not detect any association between TPC2 and the lysosome-localized proteins RagB (Figure S3A), V-ATPase (Figure S3B) or lamptors (Figure S3C, D) that interact with mTOR under certain conditions (Kim et al., 2008; Sancak et al., 2010; Zoncu et al., 2011). In contrast to TPCs, the transfected ATP-insensitive endolysosomal channel TRPMLs (Figure 2B, Figure 4A, lane 2, Figure S3E) had little or no detectable association with mTOR.

LysoNa$_{ATP}$'s ATP sensitivity was increased by ~ 5 fold when mTOR protein was increased above endogenous levels by mTOR cDNA transfection (Figure 4B, C-E). When a rapamycin-resistant mTOR (residue S2035 mutated to T, S2035T, (Vilella-Bach et al., 1999)) was co-transfected with TPC2, the resulting lysoNa$_{ATP}$ became insensitive to rapamycin (Figure 4F). Thus, mTOR determines lysoNa$_{ATP}$'s rapamycin sensitivity.

To determine whether lysoNa$_{ATP}$ requires mTOR's kinase activity, we inhibited the endogenous mTOR with rapamycin and then re-introduced mTOR activity by transfection of

a rapamycin-resistant mTOR. The mutant with an additional mutation in mTOR's catalytic domain (D2357E, kinase dead mutant (Vilella-Bach et al., 1999)), unlike wild-type, was unable to support lysoNa$_{ATP}$'s ATP sensitivity (Figure 4G, H), suggesting that mTOR's kinase activity is required. Through mutation of potential mTOR phophosites of TPC2's putative cytosolic domains, we have not located the sites of phosphorylation that are important for the channel's ATP inhibition. The functionally important mTOR residues in lysoNa$_{ATP}$ could be on cryptic sites of these TPCs or on TPC complex-associated subunits yet to be identified.

LysoNa$_{ATP}$ Detects Nutrient Depletion

In addition to sensing mM [ATP] (Dennis et al., 2001), mTOR is also a major sensor for cellular nutrients (Laplante and Sabatini, 2012b). Nutrient depletion is known to cause mTOR translocation away from lysosomal membranes (Korolchuk et al., 2011; Sancak et al., 2010), where TPC2 is localized (Calcraft et al., 2009). When cells were starved by depleting glucose and amino acids for 60 min, resulting in a drop of cellular ATP content from 3.9 ± 0.5 (n = 8) to 2.1 ± 0.3 (n = 10) nmole/10^6 cells, I_{TPC2} was no longer inhibited by ATP (Figure 5A, B, E), presumably as a result of loss of mTORC1 on the lysosomal membrane.

In nutrient-replete cells, mTORC1 is recruited to the lysosomal surface by the Rag GTPases (Kim et al., 2008; Sancak et al., 2008). When RagB^{GTP}, a GTP-bound mutant that retains mTOR on lysosomes (Sancak et al., 2008), was transfected with TPC2, the resulting lysoNa$_{ATP}$ was inhibited by ATP even after cell starvation (Figure 5 C, E). In contrast, transfection of a GDP-bound Rag mutant (RagB^{GDP}) that prevents mTOR from being localized on lysosomal surface rendered the channel insensitive to ATP even in replete cells (Figure 5D, E).

Amino acid depletion alone is sufficient to cause mTORC1's translocation away from lysosomes (Sancak et al., 2010; Sancak et al., 2008). Similarly, removal of amino acid (Figure 5G), but not glucose alone (Figure 5F), was also sufficient to render lysoNa$_{ATP}$ largely ATP-insensitive. Re-feeding nutrient-deprived cells with amino acids for 10 min, a condition sufficient to relocate mTOR back onto the lysosomal membrane after starvation (Sancak et al., 2008), quickly restored the channel's ATP sensitivity (Figure 5H, I). Consistent with the change of lysoNa$_{ATP}$'s ATP sensitivity during the course of amino acid removal and re-feeding, little mTOR was associated with TPC2 after amino acid depletion and the association was quickly restored upon amino acid re-feeding (Figure 5J).

TPC1 and TPC2 Constitute Native lysoNa$_{ATP}$

To test the *in vivo* function of TPC1 and TPC2, we generated mice with *tpc1*, *tpc2* or both *tpc1* and *tpc2* disrupted. In peritoneal macrophage endolysosomes isolated from the *tpc1*/*tpc2* double knockout (dKO), 1 μM PI(3,5)P_2 elicited no inward current (Figure 6A, B). The small residual basal currents, presumably from other channels such as TRPML1, did not contribute to the ATP-sensitivity (Figure 6B, C). The absence of lysoNa$_{ATP}$ in the double KO is not a result of potential developmental defect, as transient transfection of a human (Figure 6D, E) or mouse (Figure 6E) TPC cDNA into the mutant macrophages restored the ATP-sensitive currents. Cells from mice lacking TPC1 or TPC2 alone had measureable lysoNa$_{ATP}$, although at reduced levels (current density: *tpc1* KO, 71 ± 19 pA/pF, n = 8; *tpc2* KO, 66 ± 31 pA/pF, n = 5; WT, 130 ± 16 pA/pF, n = 12). These data suggest that lysoNa$_{ATP}$ is formed by TPC1 and/or TPC2 in the native cells and there are no other major ATP-sensitive cation channels in these organelles.

Since mTOR is a key component for the ATP sensitivity of lysoNa$_{ATP}$, we tested whether mTOR's kinase activity also required lysoNa$_{ATP}$. In cultured hepatocytes, insulin stimulated mTOR-dependent (rapamycin-sensitive) phosphorylation of a major target p70S6K in both the WT and the dKO cells (Figure S4A). Similarly, amino acid feeding stimulated mTOR translocation to the lysosome in both the WT and TPC1/2 dKO (Figure S4B). These data suggest that mTOR does not require TPCs for its function and places lysoNa$_{ATP}$ downstream of mTOR in the signaling cascade.

lysoNa$_{ATP}$ Controls Endolysosomal Na^+ Permeability, Membrane Potential and Sensitivity to ATP

The membrane potentials of endolysosomes have been only indirectly monitored using voltage-sensitive dyes. We directly measured the membrane potentials ($\Delta\Psi$, V_m, defined as $V_{cytosol} - V_{lumen}$ (Bertl et al., 1992)) using current clamp recording. Similar to that of plasma membranes, endolysosomal V_m is sensitive to K^+, Na^+, H^+, and Cl^- (Cang and Ren, unpublished). In the absence of ATP, the membrane potential of the wild-type macrophage endolysosomes was +38.0 ± 1.4 mV (lumen more negative compared to cytosol). The endolysosome expressing mutant lysoNa$_{ATP}$ was ~ 20 mV more hyperpolarized than WT (+20.5 ± 1.1 mV) (Figure 7A-C). In the WT, removal of cytosolic Na^+ led to a change in $\Delta\Psi$ of 9.7 mV (Figure 7A, C). The mutant endolysosomes' membrane potential, however, was insensitive to changes in cytosolic [Na^+] (Figure 7B, C). These data suggest that lysoNa$_{ATP}$ is a major determinant of the endolysosomal membrane's resting Na^+ permeability, similar to NALCN's (a 24 transmembrane-spanning channel with sequence similarity to that of TPCs) effect on the plasma membrane of neurons (Ren, 2011). ATP inhibition of TPCs led to a change of $\Delta\Psi$ to +19.6 ± 1.8 mV in WT but had no effect on that of the mutant (Figure 7A-C). These data suggest that lysoNa$_{ATP}$ also controls the membrane potential's ATP sensitivity: a drop of ATP leads to a depolarization of endolysosomes (lumen more negative) due to the opening of TPCs and an efflux of Na^+ from endolysosomal lumen into cytosol.

lysoNa$_{ATP}$ Regulates Lysosomal pH Stability

Membrane potentials regulate a wide spectrum of physiological processes on the plasma membrane through proteins such as voltage-gated ion channels and voltage-sensitive enzymes (Hille, 2001). It's not clear whether endolysosomes have similar voltage-sensitive proteins. One potential consequence for an increase of $\Delta\Psi$ (lumen more negative) during a decrease of available ATP is to enable the V-ATPase to maintain lysosomal pH at the pump's set point. Consistent with this idea, WT lysosomes maintained a relatively stable pH upon starvation (4.73 ± 0.01 before, and 4.74 ± 0.01 after starvation). In contrast, there was a significant shift of pH toward alkalization in the mutant (4.82 ± 0.01 before, and 5.36 ± 0.02 after starvation; Figure 7D-F).

lysoNa$_{ATP}$ Is Required for Normal Amino Acid Homeostasis during Starvation Stress

A potential function for lysoNa$_{ATP}$'s control of lysosomal V_m and pH is to regulate the fusion between autophagosomes and lysosomes, one of the last steps of macroautophagy during which nutrients such as amino acids can be generated in response to starvation (Mizushima and Komatsu, 2011). The mutant mice, however, do not appear to have gross defects in autophagy (Figure S5A-C). During food deprivation stress, one of the homeostatic responses is an increase in the levels of certain amino acids in the circulation, partly due to protein digestion in the lysosomes and the subsequent export of amino acids from these organelles (Brady et al., 1978; Cahill, 2006). The transport of amino acids, particularly cations (lysine and arginine), by the lysosomal system *c* transportation system, is likely influenced by lysosomal membrane potential and pH (Pisoni and Thoene, 1991). We loaded liver lysosomes with ^{14}C-labeled lysine and monitored the efflux at various time points.

With 2 mM ATP in the efflux buffer, sufficient to inhibit lysoNa$_{ATP}$, there was no significant efflux rate difference between WT and the dKO. With [ATP] reduced to 0.1 mM, a condition under which lysoNa$_{ATP}$ is open, the amino acid efflux was significantly faster in the WT lysosomes than in the dKO (Figure S5D). We also measured the levels of circulating amino acids 6 hr and 3 days after the onset of food deprivation in the WT and dKO mice. In WT mice, the levels of plasma lysine and arginine increased by 26% and 67%, respectively, upon prolonged fasting (Figure 7G). In the mutant, such increases were largely absent. Changes in the levels of total amino acids were less compromised in the mutant (WT, 38%; dKO, 7%; $p = 0.06$, Figure 7G).

lysoNa$_{ATP}$ Is Required for Normal Fasting Endurance

Under normal in-house conditions, *tpc1*/*tpc2* dKO adult mice are viable, fertile, have no obvious morphological abnormalities, and no obvious behavioral defects (observation, and as measured with rotarod and treadmill tests; Figure 7H, I). Since lysoNa$_{ATP}$ opens primarily when [ATP] is low or when nutrients are restricted, we subjected the mice to food deprivation. After fasting for 3 days, WT mice remained alert and active in food search activities. Endurance performance in the treadmill test was comparable to, or better (5/10) than that before fasting, consistent with the findings of fasting-induced hyperactivity found in animal behavioral tests (Challet et al., 1997; Yamanaka et al., 2003). In contrast, dKO mice were less active after fasting, endurance performance was reduced by 8.3 fold, and none performed better than before fasting (Figure 7H, I). Two days after re-introduction of food, dKO mice regained endurance and became as active as before fasting (Figure 7I). In the less strength-demanding rotarod test, the mutant's performances were less affected by fasting (Figure S5E).

DISCUSSION

We have shown that mTOR associates with the channel pore of lysoNa$_{ATP}$, formed by TPC proteins, and controls channel activation. Nutrient replete cells have high [ATP], which presumably enables mTOR to phosphorylate TPC and/or its associated proteins and maintain the channel in the closed state. During cell starvation, ATP levels fall, mTOR delocalizes from TPC, and lysoNa$_{ATP}$ opens, allowing Na^+ and other ions to leave the lysosome. Thus, TPCs link lysosomal control of nutrient recycling to the extensive signaling mTOR network that monitors and responds to nutrient depletion, hypoxia and cell growth (Laplante and Sabatini, 2012b). Intracellular ATP concentrations are normally a few mM at rest but vary among cell types, during different metabolic conditions, and during circadian cycles. These levels can drop to < 0.1 mM during starvation, hyperosmotic stress, hypoxia and ischemia (Berg et al., 2009; Gribble et al., 2000; Imamura et al., 2009; Isidoros and Newsholme, 1975). With its ATP sensitivity tuned to the range of physiological concentrations and regulated by nutrient availability, lysoNa$_{ATP}$ couples the cell's energy status to endolysosomal function. In a natural environment, an animal's survival depends on its ability to deal with stress, to maintain the ability to search for food, and to fend off attacks from intruders even during frequent starvation. TPC's evolutionally conserved endolysosomal function in fasting endurance presumably serves this purpose.

Currently, we do not know how the channel affects lysosomal regulation of such functions as protein degradation, energy generation, plasma membrane repair and exocytosis to maintain cell viability (Laplante and Sabatini, 2012b; Luzio et al., 2007; Settembre et al., 2011). Plasma membrane potentials control many physiological responses ranging from fertilization, muscle contraction, neuronal excitability, synaptic transmission, hormone release, to immune responses. Opening of lysoNa$_{ATP}$ depolarizes endolysosomal membranes, but how voltage changes across endolysosomal membranes are detected is

poorly understood. The membrane potential has controls on the basic endolysosomal properties such as pH and amino acid transportation (Figure 5; (Pisoni and Thoene, 1991)), and this will require extensive new experiments. TPCs and mTORC1 are widely expressed in many organs including brain, heart, intestine, liver and pancreas. As such, the cell types and circuitry in which lysoNa$_{ATP}$ functions to regulate the fasting endurance need to be determined.

Originally proposed to be activated by NAADP (Calcraft et al., 2009), recent data suggest that NAADP binds to proteins other than TPC1/2 (Lin-Moshier et al., 2012; Walseth et al., 2012) and do not activate TPCs (Figure S1F, G; see also (Wang et al., 2012)). I_{TPC} is also recently shown to be potentiated by PI(3,5)P_2 under isolated endolysosome recording conditions (Wang et al., 2012). It is not known whether PI(3,5)P_2 is a basal requirement for the channel activity under physiological conditions, similar to the requirement of PI(4,5)P_2 for many plasma membrane ion channels and transporters, or if there is significant change of PI(3,5)P_2 levels during signaling to potentiate TPCs. Nevertheless, the ATP sensitivity of lysoNa$_{ATP}$ is independent of PI(3,5)P_2 since basal TPC current in the absence of added PI(3,5)P_2 is similarly regulated by ATP.

The mTOR complexes are master integrators linking cellular metabolism to many adaptive cellular responses such as global gene expression (Laplante and Sabatini, 2012b). The targets of mTOR are primarily cytosolic and mTOR is predominantly localized on endolysosomal membranes under physiological conditions (Korolchuk et al., 2011; Sancak et al., 2010; Zoncu et al., 2011). One functional consequence of the recruitment of mTOR to the lysosomal membrane is to detect amino acid content inside the lysosomes for the subsequent action on transcriptional cascades important for cellular responses such as lysosomal biogenesis (Han et al., 2012; Sancak et al., 2010; Settembre et al., 2011; Zoncu et al., 2011). Our data suggest that mTOR not only directly receives information from lysosomes but also acutely controls endosomal and lysosomal functions through lysoNa$_{ATP}$ in response to changes in the cell's energy and nutrient status. Dysregulation of mTOR and the components in its signaling network is linked to many diseases such as diabetes, cancer, neurodegeneration, seizure and autism. Since both mTOR and lysoNa$_{ATP}$ are widely expressed, lysoNa$_{ATP}$ channels may enable more precise downstream targeting in mTOR-associated disorders.

EXPERIMENTAL PROCEDURES

Animals

Animal uses followed NIH guidelines and were approved by the IACUC at the University of Pennsylvania. To generate *tpc1* and *tpc2* knockouts, the exons containing the translational start site (ATG) were deleted. The mutant TPC1 and TPC2 proteins are predicted to lack the first 69 and 49 amino acids, respectively, and do not generate detectable current, as tested in HEK293T cells (Wang et al., 2012) and in the *tpc1*/*tpc2* double knockout cells (Figure 6). We cannot rule out the possibility that small, undetectable residual channels formed by the mutant proteins can support functions such as animal viability. Individual knockouts were backcrossed to C57BL6/J for 4 (*tpc1*) or 6 (*tpc2*) generations before being used to generate the double knockout (dKO).

cDNA Constructs, Transfection and Cell Culture

Unless otherwise stated, all the channel clones were GFP-tagged for the identification of channel protein-expressing endolysosomes used for patch clamp recordings. Cell culture, transfection and the used ion channel and mTOR cDNA clones are described in Extended Experimental Procedures.

Knockdown of mTOR, Raptor and Rictor

Infection with lentivirus encoding shRNA of mTOR, Raptor and Rictor was used for long-term knockdown of the target proteins (Sarbassov et al., 2005). To generate lentivirus, HEK293T cells were transfected with shRNA plasmids (Addgene plasmid 1855 (mTOR), 1857 (Raptor) and 1853 (Rictor), in pLKO.1 vector), lentivirus packing plasmid psPAX2 and envelope plasmid pMD2.G (gifts from Dr. Didier Trono), using Fugene 6 reagent (Roche Applied Bioscience). Two days after transfection, medium containing lentivirus particles was collected and added into a new dish of HEK293T cells cultured in antibiotics-free medium. Polybrene (8 g/ml, Sigma-Aldrich) was added to increase the efficiency of viral infection. Infected cells were selected with puromycin (3 μg/ml, Sigma-Aldrich) starting the day after infection. Protein expression was tested using Western blot 4 days after infection. For patch clamp recordings, TPC2 plasmid was transfected into the cells at least 2 days after infection and recorded two days later. Control lentivirus encoding scrambled shRNA (generated from Addgene plasmid #1864) was used as a negative control.

Protein Chemistry and Immunohistochemistry

Details of Western blotting and immunohistochemistry are described in Extended Experimental Procedures.

ATP Measurement

ATP levels in HEK293T cells were measured using luminescence ATP detection kit (ATPlite, PerkinElmer). Luminescence signals were detected using an Analyst HT plate reader (Molecular Device Corporation). ATP levels were calculated from standard curves.

Amino Acid Analysis

Plasma samples were obtained from heparinized blood by centrifugation. The concentration of amino acids in the plasma was determined with an Agilent 1260 Infinity LC system utilizing precolumn derivatization with o-phthalaldehyde, as previously described (Jones and Gilligan, 1983).

Lysosome pH Imaging

Ratiometric lysosome pH measurements were carried out as previously described (Steinberg et al., 2010). Briefly, peritoneal macrophages were placed on glass coverslip and loaded overnight with Oregon-Green 488, Dextran pH-sensitive dye (250 μg/ml, Invitrogen, #D7170) in culture medium. For control groups, cells were washed once and chased for 2 h at 37°C in culture medium. For starvation groups, cells were washed once in starvation buffer (in mM, 110 NaCl, 45 $NaHCO_3$, 5 KCl, 2 $CaCl_2$, 1 $MgCl_2$, pH7.4) and chased for 2 h in the same buffer at 37°C. Fluorescence images were acquired using an inverted microscope (Olympus IX71 equipped with a 60x water immersion lens) connected to a DeltaRAM V monochromator (PTI). Excitation wavelengths were 440 nm and 490 nm.

Emissions were filtered (545 ± 50 nm) and acquired with an EMCCD camera (Evolve 512, Photometrics) controlled with Metamorph software (Molecular Devices). Modified Ringer solution (in mM: 140 NaCl, 3 KCl, 2 K2HPO4, 1 CaCl2, 1 MgSO4, 5 HEPES, 10 glucose, 1X amino acid mix, pH 7.4) was used during pH imaging, and 1X amino acid mix was omitted for starvation group. The mean intensity ratio (490/440) was calculated for each individual lysosome. At the end of imaging for each coverslip, in situ pH calibration was performed in isotonic K^+ solutions (5 mM NaCl, 115 mM KCl, 1.2 mM $MgSO_4$, 10 mM Glucose, 25 mM HEPES, supplemented with 10 μM of nigericin and monensin, pH ranging from 4.0 to 7.0). Following 5 min of incubation for the equilibration of pH across lysosome membranes, pH images were acquired for each standard solution. The resulting fluorescence

intensity ratios (F_{490}/F_{440}) as a function of pH were fitted to a Boltzmann sigmoid. Lysosome pH values were obtained by fitting the intensity ratios obtained during the experiment to the standard curves.

Lysosomal Amino Acid Efflux Measurement

Amino acid efflux was measured using liver lysosomes loaded with ^{14}C-labeled amino acid methyl ester, as described in Extended Experimental Procedures.

Electrophysiology

Whole endolysosome recordings followed the previously described method (Saito et al., 2007) except that endolysosomes were enlarged with the treatment of vacuolin −1 (1 μM (Dong et al., 2008)) for 1-6 h (macrophages and cardiac myocytes) or overnight (hepatocytes, fibroblasts and HEK293T cells). Briefly, the cell membrane was cut with a glass pipette at a position close to the endolysosome to be patched. Endolysosomes were pushed out through the cut position with the pipette tip. In cells transfected with GFP-tagged TPC or TRPML, only the GFP-positive endolysosomes were selected for recording. Only one endolysosome was recorded from each coverslip. Patch recordings were performed with a Multiclamp 700B amplifier (Molecular Device) and a Digidata 1440A data acquisition system (Molecular Device). PClamp and Clampfit software was used to record and analyze data. Recording pipettes of borosilicate glass had resistances of 3-6 ΩM . For voltage-clamp recordings, bath solution (cytosolic) contained (in mM) 140 K-gluconate, 4 NaCl, 2 $MgCl_2$, 0.39 $CaCl_2$, 1 EGTA and 10 HEPES (pH adjusted to 7.2 with KOH). Pipette solution (luminal) contained (in mM) 145 NaCl, 5 KCl, 1 $MgCl_2$, 2 $CaCl_2$, 10 HEPES, 10 MES and 10 glucose (pH adjusted to 4.6 with NaOH) (Dong et al., 2010; Wang et al., 2012). For current-clamp recordings, bath solution contained (in mM) 10 Nagluconate, 130 K-gluconate, 4 KCl, 2 $MgCl_2$, 0.39 $CaCl_2$, 1 EGTA, 0.0001 $PI(3,5)P_2$ and 10 HEPES (pH adjusted to 7.2 with KOH) and pipette solution was consisted of (in mM) 70 NaCl, 70 KCl, 1 $MgCl_2$, 2 $CaCl_2$, 10 HEPES, 10 MES and 10 glucose (pH adjusted to 4.6 with NaOH). In 0-Na bath, Na-gluconate was substituted with K-gluconate. Liquid junction potential was corrected. Unless otherwise stated, recordings were obtained in the presence of 1 μM $PI(3,5)P_2$ (water-soluble diC8 form, from Echelon Biosciences) in the bath. ATP-Mg was used for the ATP inhibition experiment. Nucleotide solutions used for bath application were pH-adjusted. ATP inhibition curves were fitted with the equation: $I/I_0=(I_R/I_0)+[1-(I_R/I_0)]/[1+([ATP]/IC_{50})^h]$, where I and I_0 are the currents obtained in the presence and absence of ATP, respectively. I_R is the residual current. IC_{50} is the ATP concentration required for half-maximal inhibition, and h is the Hill coefficient. Only the endolysosomes with currents > 200 pA (at −100 mV, without ATP) were selected for the curve fitting.

Behavior Tests

Rotarod and treadmill tests were performed as described in Extended Experimental Procedures.

Data Analysis

Data was analyzed using Clampfit (Molecular Device), Origin (Origin Lab) and Excel (Microsoft). Values of data were shown as mean ± s.e.m. Statistical analysis was performed using Student's t-test. Significant difference was considered when $p < 0.05$.

Supplementary Material

Refer to Web version on PubMed Central for supplementary material.

Acknowledgments

We thank members of the Ren lab for discussion, Amita Tiyaboonchai for starting our interest in macrophages, Drs. Morris Birnbaum and Russell Miller for AMPK1/2 dKO MEF cells, Dr. Sara Cherry for the use of plate reader, Dr. Jie Chen for mTOR and S6K1 clones, and Dr. Denia Ramirez-Montealegre for advice on amino acid efflux assay. This work was supported, in part, by funding from American Heart Association, NIH and the University of Pennsylvania Research Foundation. ES cell injections were performed in the Gene Manipulation Facility of the Children's Hospital Boston (*tpc1*) and the Transgenic and the Chimeric Mouse Facility at University of Pennsylvanian (*tpc2*). Amino acid measurement was performed by Ilana Nissim in the Metabolomic Core Facility, Children's Hospital of Philadelphia Research Institute (supported in part by NIH grant number DK-053761).

REFERENCES

Baukrowitz T, Schulte U, Oliver D, Herlitze S, Krauter T, Tucker SJ, Ruppersberg JP, Fakler B. PIP2 and PIP as determinants for ATP inhibition of KATP channels. Science. 1998; 282:1141–1144. [PubMed: 9804555]

Berg J, Hung YP, Yellen G. A genetically encoded fluorescent reporter of ATP:ADP ratio. Nat Methods. 2009; 6:161–166. [PubMed: 19122669]

Bertl A, Blumwald E, Coronado R, Eisenberg R, Findlay G, Gradmann D, Hille B, Kohler K, Kolb H-A, MacRobbie E, et al. Electrical measurements on endomembranes. Science. 1992; 258:873–874. [PubMed: 1439795]

Brady JJ, Romsos DR, Brady PS, Bergen WG, Leveille GA. The effects of fasting on body composition, glucose turnover, enzymes and metabolites in the chicken. J Nutr. 1978; 108:648–657. [PubMed: 632952]

Brailoiu E, Churamani D, Cai X, Schrlau MG, Brailoiu GC, Gao X, Hooper R, Boulware MJ, Dun NJ, Marchant JS, Patel S. Essential requirement for two-pore channel 1 in NAADP-mediated calcium signaling. J Cell Biol. 2009; 186:201–209. [PubMed: 19620632]

Cahill GF. Fuel metabolism in starvation. Annu Rev Nutr. 2006; 26:1–22. [PubMed: 16848698]

Calcraft PJ, Ruas M, Pan Z, Cheng X, Arredouani A, Hao X, Tang J, Rietdorf K, Teboul L, Chuang K-T, et al. NAADP mobilizes calcium from acidic organelles through two-pore channels. Nature. 2009; 459:596–600. [PubMed: 19387438]

Cerny J, Feng Y, Yu A, Miyake K, Borgonovo B, Klumperman J, Meldolesi J, McNeil PL, Kirchhausen T. The small chemical vacuolin-1 inhibits Ca2+-dependent lysosomal exocytosis but not cell resealing. EMBO Rep. 2004; 5:883–888. [PubMed: 15332114]

Challet E, Pevet P, Malan A. Effect of prolonged fasting and subsequent refeeding on free-running rhythms of temperature and locomotor activity in rats. Behav Brain Res. 1997; 84:275–284. [PubMed: 9079792]

Dennis PB, Jaeschke A, Saitoh M, Fowler B, Kozma SC, Thomas G. Mammalian TOR: a homeostatic ATP sensor. Science. 2001; 294:1102–1105. [PubMed: 11691993]

Dong XP, Cheng X, Mills E, M. D, Wang F, Kurz T, Xu H. The type IV mucolipidosis-associated protein TRPML1 is an endolysosomal iron release channel. Nature. 2008; 455:992–996. [PubMed: 18794901]

Dong XP, Shen D, Wang X, Dawson T, Li X, Zhang Q, Cheng X, Zhang Y, Weisman LS, Delling M, Xu H. PI(3,5)P_2 controls membrane trafficking by direct activation of mucolipin Ca^{2+} release channels in the endolysosome. Nat Commun. 2010; 1:38. [PubMed: 20802798]

Foster DB, Rucker JJ, Marban E. Is Kir6.1 a subunit of mitoK_{ATP} ? Biochem Biophys Res Commun. 2008; 366:649–656. [PubMed: 18068667]

Glick D, Zhang W, Beaton M, Marsboom G, Gruber M, Simon MC, Hart J, G.W. D, Brady MJ, Macleod KF. BNip3 regulates mitochondrial function and lipid metabolism in the liver. Mol Cell Biol. 2012; 32:2570–2584. [PubMed: 22547685]

Gribble FM, Loussouarn G, Tucker SJ, Zhao C, Nichols CG, Ashcroft FM. A novel method for measurement of submembrane ATP concentration. J Biol Chem. 2000; 275:30046–30049. [PubMed: 10866996]

Grimm C, Jörs S, Guo Z, Obukhov AG, Heller S. Constitutive activity of TRPML2 and TRPML3 channels versus activation by low extracellular sodium and small molecules. J Biol Chem. 2012; 287:22701–22708. [PubMed: 22753890]

Han JM, Jeong SJ, Park MC, Kim G, Kwon NH, Kim HK, Ha SH, Ryu SH, Kim S. Leucl-tRNA synthetase is an intracellular leucine sensor for the mTORC1-signaling pathway. Cell. 2012; 149:410–424. [PubMed: 22424946]

Hardie DG, Ross FA, Hawley SA. AMPK: a nutrient and energy sensor that maintains energy homeostasis. Nat Rev Mol Cell Biol. 2012; 13:251–262. [PubMed: 22436748]

Hilgemann DW, Feng S, Nasuhoglu C. The complex and intriguing lives of PIP2 with ion channels and transporters. Sci STKE. 2001; 11:re19. [PubMed: 11734659]

Hille, B. Ion Channels of Excitable Membranes. ed. 3 edn. Sinauer Associates, Inc.; Sunderland, MA: 2001.

Imamura H, Nhat KPH, Togawa H, Saito K, R. L, Kato-Yamada Y, Nagai T, Noji H. Visualization of ATP levels inside single living cells with flurorescence resonance energy transfer-based genetically encoded indicators. Proc Natl Acad Sci U S A. 2009; 106:15651–15656. [PubMed: 19720993]

Inoue I, Magase H, Kishi K, Higuti T. ATP-sensitive K^+ channels in the mitochondrial inner membrane. Nature. 1991; 351:244–247. [PubMed: 1857420]

Ishibashi K, Suzuki M, Imai M. Molecular cloning of a novel form (two-repeat) protein related to voltage-gated sodium and calcium channels. Biochem Biophys Res Commun. 2000; 270:370–376. [PubMed: 10753632]

Isidoros B, Newsholme EA. The contents of adenine nucleotides, phosphagens and some glycolytic intermediates in resting muscles from vertebrates and invertebrates. Biochem J. 1975; 152:23–32. [PubMed: 1212224]

Jones BN, Gilligan JP. o-Phthaldialdehyde precolumn derivatization and reversed-phase high-performance liquid chromatography of polypeptide hydrolysates and physiological fluids. J Chromatogr. 1983; 266:471–482. [PubMed: 6630358]

Kim E, Goraksha-Hicks P, Li L, Neufeld TP, Guan K-L. Regulation of TORC1 by Rag GTPases in nutrient response. Nat Cell Biol. 2008; 10:935–945. [PubMed: 18604198]

Korolchuk VI, Saiki S, Lichtenberg M, Siddiqi FH, Roberts EA, Imarisio S, Jahreiss L, Sarkar S, Futter M, Menzies FM, et al. Lysosomal positioning coordinates cellular nutrient responses. Nat Cell Biol. 2011; 13:453–460. [PubMed: 21394080]

Laplante M, Sabatini DM. mTOR Signaling. Cold Spring Harb Perspect Biol. 2012a; 4

Laplante M, Sabatini DM. mTOR Signaling in growth control and disease. Cell. 2012b; 149:274–293. [PubMed: 22500797]

Lin-Moshier Y, Walseth TF, Churamani D, Davidson SM, Slama JT, Hooper R, Brailoiu E, Patel S, Marchant JS. Photoaffinity labeling of nicotinic acid adenine dinucleotide phosphate (NAADP) targets in mammalian cells. J Biol Chem. 2012; 287:2296–2307. [PubMed: 22117075]

Luzio JP, Pryor PR, Bright NA. Lysosomes: fusion and function. Nat Rev Mol Cell Biol. 2007; 8:622–632. [PubMed: 17637737]

McTaggart JS, R.H. C, Ashcroft FM. The role of the KATP channel in glucose homeostasis in health and disease: more than meets the islet. J Physiol. 2010; 588:3201–3209. [PubMed: 20519313]

Mizushima N, Komatsu M. Autophagy: renovation of cells and tissues. Cell. 2011; 147:728–741. [PubMed: 22078875]

Nichols CG. KATP channels as molecular sensors of cellular metabolism. Nature. 2006; 440:470–476. [PubMed: 16554807]

Noma A. ATP-regulated K^+ channels in cardiac muscle. Nature. 1983; 305:147–149. [PubMed: 6310409]

Oakhill JS, Scott JW, Kemp BE. AMPK functions as an adenylate charge-regulated protein kinase. Trends Endocrinol Metab. 2012; 23:125–132. [PubMed: 22284532]

Pisoni RL, Thoene JG. The transport systems of mammalian lysosomes. Biochim Biophys Acta. 1991; 1071:351–373. [PubMed: 1751541]

Pryor PR, Reimann F, Gribble FM, Luzio JP. Mucolipin-1 is a lysosomal membrane protein required for intracellular lactosylceramid traffic. Traffic. 2006; 7:1388–1398. [PubMed: 16978393]

Ren D. Sodium leak channels in neuronal excitability and rhythmic behaviors. Neuron. 2011; 72:899–911. [PubMed: 22196327]

Saito M, Hanson P, Schlesinger P. Luminal chloride-dependent activation of endosome calcium channels: patch clamp study of enlarged endosomes. J Biol Chem. 2007; 282:27327–27333. [PubMed: 17609211]

Sancak Y, Bar-Peled L, Zoncu R, Markhard AL, Nada S, Sabatini DM. Ragulator-Rag complex targets mTORC1 to the lysosomal surface and is necessary for its activation by amino acids. Cell. 2010; 141:290–303. [PubMed: 20381137]

Sancak Y, Peterson TR, Shaul YD, Lindquist RA, Thoreen CC, Bar-Peled L, Sabatini DM. The Rag GTPases bind raptor and mediate amino acid signaling to mTORC1. Science. 2008; 320:1496–1501. [PubMed: 18497260]

Sarbassov DD, Guertin DA, Ali SM, Sabatini DM. Phosphorylation and regulation of Akt/PKB by the rictor-mTOR complex. Science. 2005; 307:1098–1101. [PubMed: 15718470]

Settembre C, Di Malta C, Polito VA, Garcia Arencibia M, Vetrini F, Erdin S, Erdin SU, Huynh T, Medina D, Colella P, et al. TFEB links autophagy to lysosomal biogenesis. Science. 2011; 332:1429–1433. [PubMed: 21617040]

Shyng S-L, Nichols CG. Membrane phospholipid control of nucleotide sensitivity of KATP channels. Science. 1998; 282:1138–1141. [PubMed: 9804554]

Steinberg BE, Huynh KK, Brodovitch A, Jabs S, Stauber T, Jentsch TJ, Grinstein S. A cation counterflux supports lysosoml acidification. J Cell Biol. 2010; 189:117–1186.

Suh BC, Hille B. PIP2 is a necessary cofactor for ion channel function: how and why? Annu Rev Biophys. 2008; 37:175–195. [PubMed: 18573078]

Vilella-Bach M, Nuzzi P, Fang Y, Chen J. The FKBP12-Rapamycin-binding Domain Is Required for FKBP12-Rapamycin-associated Protein Kinase Activity and G_1 Progression. J Biol Chem. 1999; 274:4266–4277. [PubMed: 9933627]

Walseth TF, Lin-Moshier Y, Jain P, Ruas M, Parrington J, Galione A, Marchant JS, Slama JT. Photoaffinity labeling of high affinity nicotinic acid adenine dinucleotide phosphate (NAADP)-binding proteins in sea urchin egg. J Biol Chem. 2012; 287:2308–2315. [PubMed: 22117077]

Wang X, Zhang X, Dong XP, Samie M, Li X, Cheng X, Goschka A, Shen D, Zhou Y, Harlow J, et al. TPC proteins are phosphoinositide-activated sodium-selective ion channels in endosomes and lysosomes. Cell. 2012; 151:372–383. [PubMed: 23063126]

Wu L, Bauer CS, X.G. Z, Xie C, Yang J. Dual regulation of voltage-gated calcium channels by PtdIns(4,5)P2. Nature. 2002; 419:947–952. [PubMed: 12410316]

Yamanaka A, Beuckmann CT, Willie JT, Hara J, Tsujino N, Mieda M, Tominaga M, Yagami K-I, Sugiyama F, Goto K, et al. Hypothalamic orexin neurons regulate arousal according to energy balance in mice. Neuron. 2003; 38:701–713. [PubMed: 12797956]

Zoncu R, Bar-Peled L, Efeyan A, Wang S, Sancak Y, Sabatini DM. mTORC1 senses lysosomal amino acids through an inside-out mechanism that requires the vacuolar H^+-ATPase. Science. 2011; 334:678–683. [PubMed: 22053050]

HIGHLIGHTS

- Lysosomes detect [ATP] via a novel Na^+ channel ($lysoNa_{ATP}$) formed by TPCs and mTOR.
- TPC channels are not gated by NAADP as previously thought.
- $lysoNa_{ATP}$ detects extracellular nutrients via mTOR.
- $lysoNa_{ATP}$ regulates lysosomal pH stability and animal's fasting endurance.

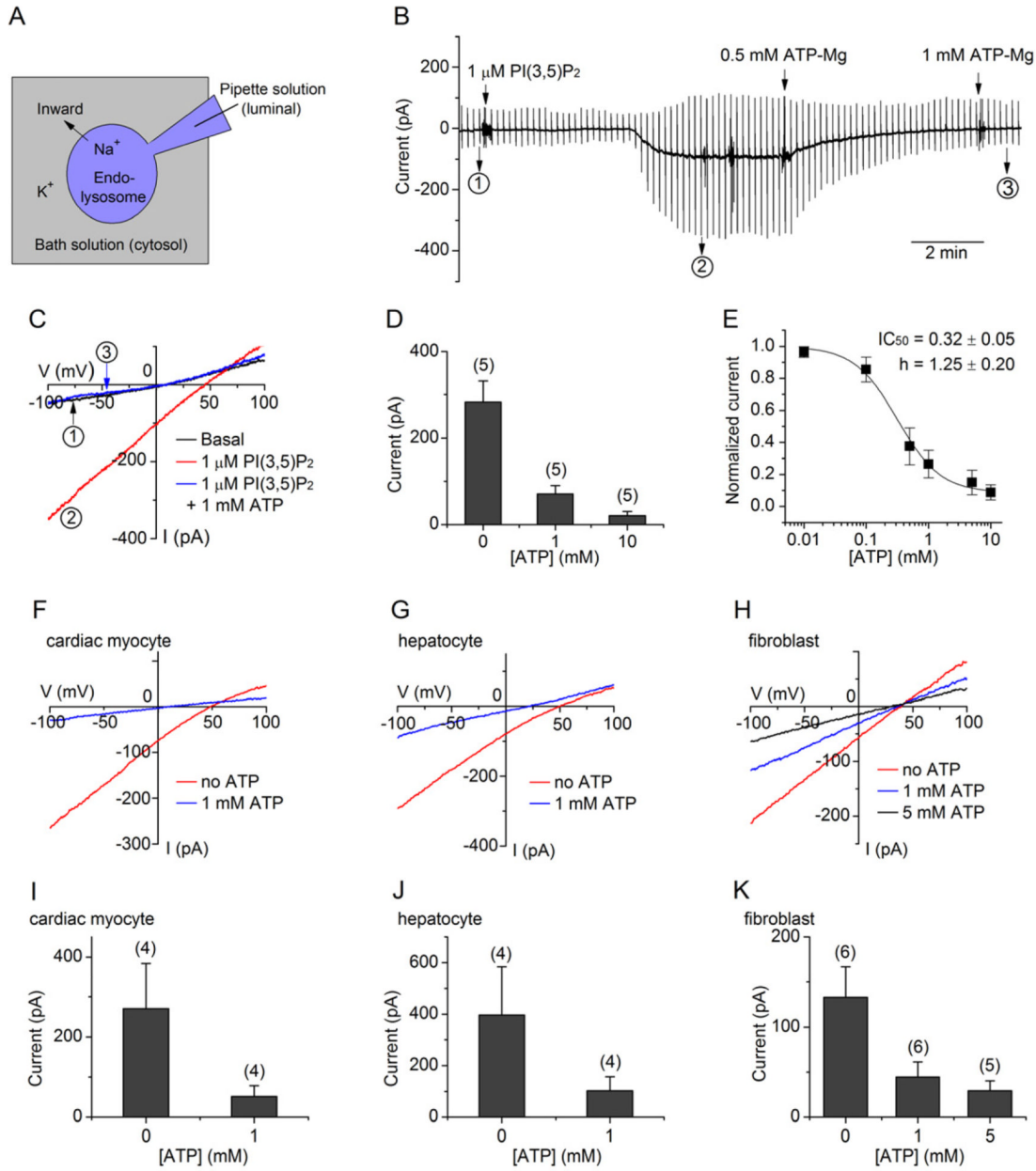

Figure 1. Endolysosomal ATP-sensitive Channel (lysoNa$_{ATP}$)

(A) Whole-endolysosome patch clamp recording. Inward current (negative) denotes positive charge flowing into the cytosol (bath) from the endolysosomal lumen. (B-E) Recordings with ramp protocols (−100 to +100 mV in 1 s, every 10 s, V_h = 0 mV) from mouse peritoneal macrophages. (B) Representative continuous recordings. Recordings at time points *1*, *2* and *3* (indicated) were used for the current-voltage (I-V) relationships in (C). (D) Statistics of current amplitudes at -100 mV. (E) Current amplitudes normalized to those obtained without ATP and fitted to the Hill equation (n ≥ 5). (F-K) Representative (F-H) and averaged (I-K) ATP-sensitive currents recorded from cardiac myocytes (F, I), hepatocytes (G, J) and fibroblasts (H, K). Unless otherwise stated, recordings shown were obtained with $PI(3,5)P_2$ (1 μM) in the bath. Numbers of endolysosomes are in parentheses. Data are presented as mean ± SEM.

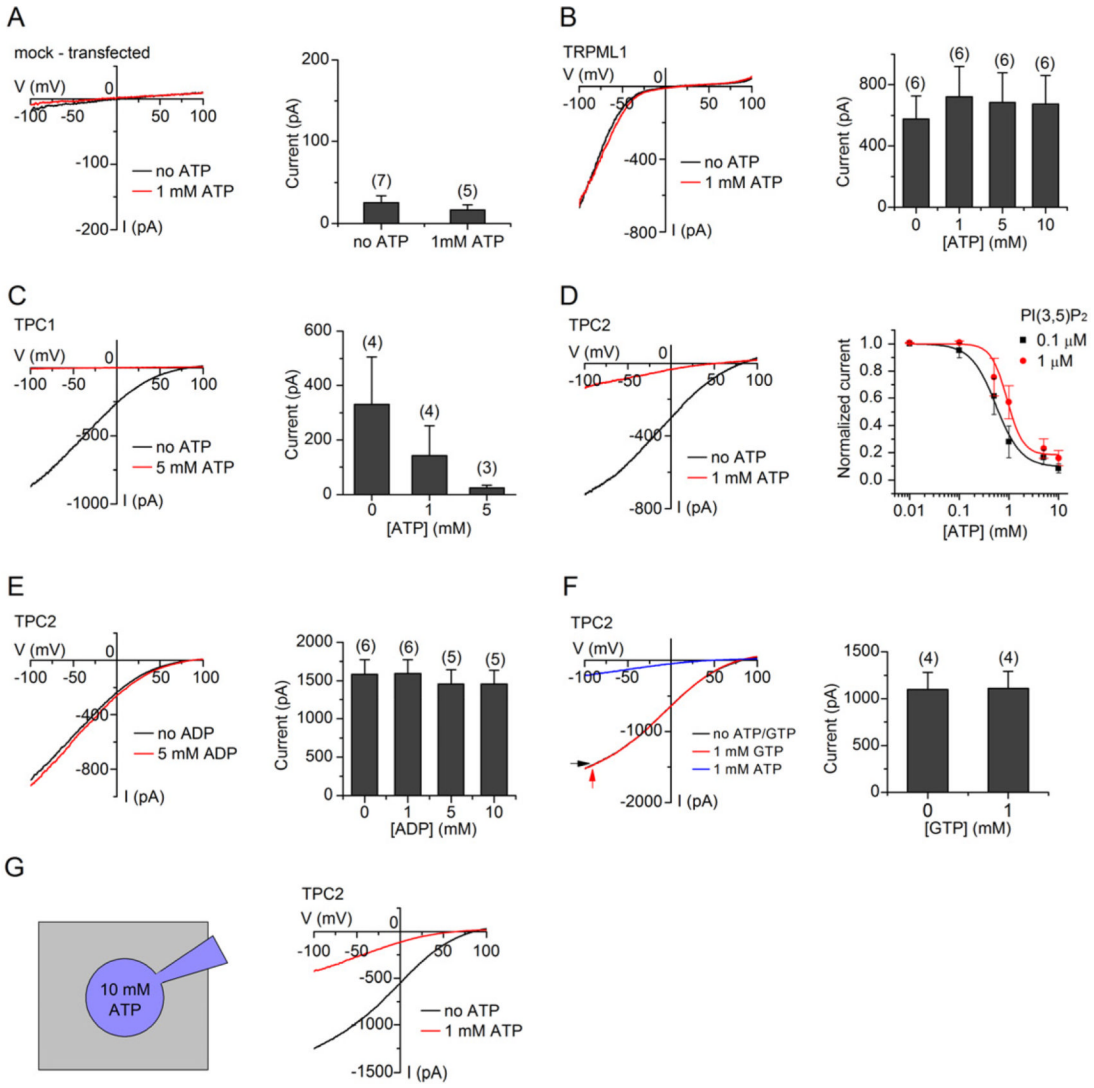

Figure 2. TPC1 and TPC2 Form lysoNa$_{ATP}$ in HEK293T Cells

(**A-D**) ATP sensitivity of endolysosomal currents was tested in HEK293T cells transfected with GFP (A) or GFP-tagged TRPML1 (B), TPC1 (C) and TPC2 (D). PI(3,5)P_2 (1 μM) was included in the bath during recordings. (A) Mock-transfected HEK293T cells had little lysoNa$_{ATP}$ current (24.9 ± 8.7 pA without ATP, 16.2 ± 6.2 pA with 1 mM ATP-Mg, at -100 mV). (B) I_{TRPML1} is insensitive to ATP, as shown in the representative recordings (*left*) and the statistics of the averaged current amplitudes (*right*, at −100 mV). (C, D) ATP-sensitive currents recorded from TPC1- (C) and TPC2-transfected cells (D). The IC_{50} of ATP on I_{TPC2} was 0.55 ± 0.09 mM and 0.92 ± 0.31 mM in presence of 0.1 μM and 1 μM PI(3,5)P_2, respectively (n ≥ 4). (E, F) I_{TPC2} is insensitive to ADP (E) and GTP (F). (G) Similar to (*D*) but 10 mM ATP-Mg was added to the pipette solution. Data are shown as mean ± SEM. See also Figure S1.

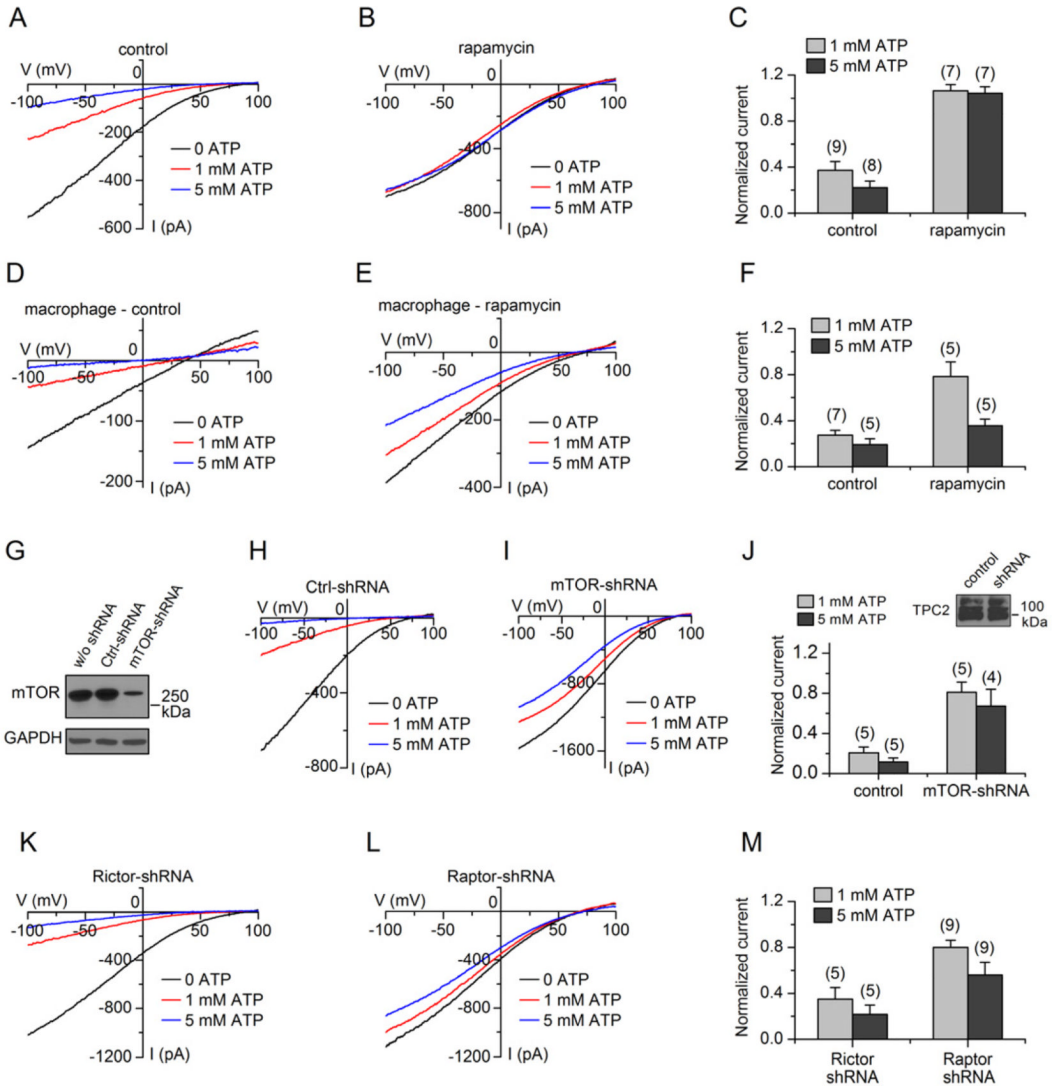

Figure 3. mTOR Is Required for lysoNa$_{ATP}$'s ATP Sensitivity

(A-C) Compared with the control (*A*, no rapamycin), currents from TPC2-transfected endolysosomes were minimally inhibited by 1 mM ATP in the presence of rapamycin (*B*, 0.2 μM rapamycin). Statistical data are in (C). (D-F) Similar to (A-C), but recorded from macrophages (1.0 μM rapamycin used in *E*). (G-J) Infecting HEK293T cells with shRNA lentivirus against mTOR but not with the control shRNA reduced the endogenous mTOR protein level (G) and TPC2 current's ATP sensitivity (H-J). Inset in (J) indicates TPC2 protein levels in control and mTOR shRNA virus-infected cells. (K-L) Knocking down Raptor (L) but not Rictor (K) reduced lysoNa$_{ATP}$'s ATP sensitivity. Data are represented as mean ± SEM. See also Figure S2.

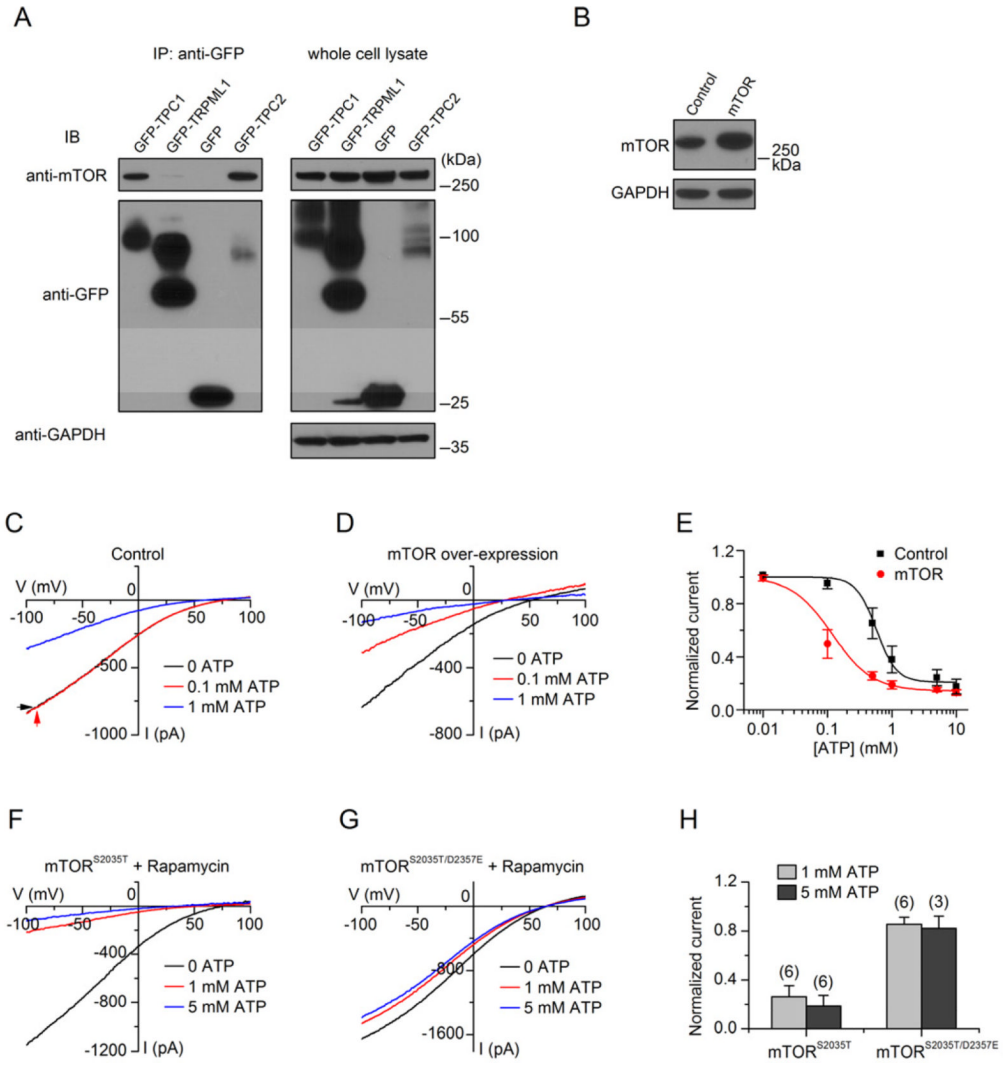

Figure 4. TPCs Form a Complex with mTOR

(A) Immunoblotting (IB) with whole cell lysates or immunoprecipitates (IP) from cells co-transfected with mTOR and GFP or GFP-tagged channels as indicated, showing that both TPC1 and TPC2, but not TRPML1, associate with mTOR. (B-E) Co-transfecting mTOR and TPC2 into HEK293T cells increased mTOR protein levels (B) and TPC2's ATP sensitivity, as shown in representative recordings (C, D) and normalized current sizes at −100 mV (E). (F-H) lysoNa$_{ATP}$ currents recorded in the presence of rapamycin (1 μM) from cells co-transfected with a rapamycin-resistant mTOR (mTOR^{S2035T}) (F, H), or a rapamycin-resistant and kinase dead double mutant (mTOR$^{S2035T/D2357E}$) (G, H). Data are presented as mean ± SEM. See also Figure S3.

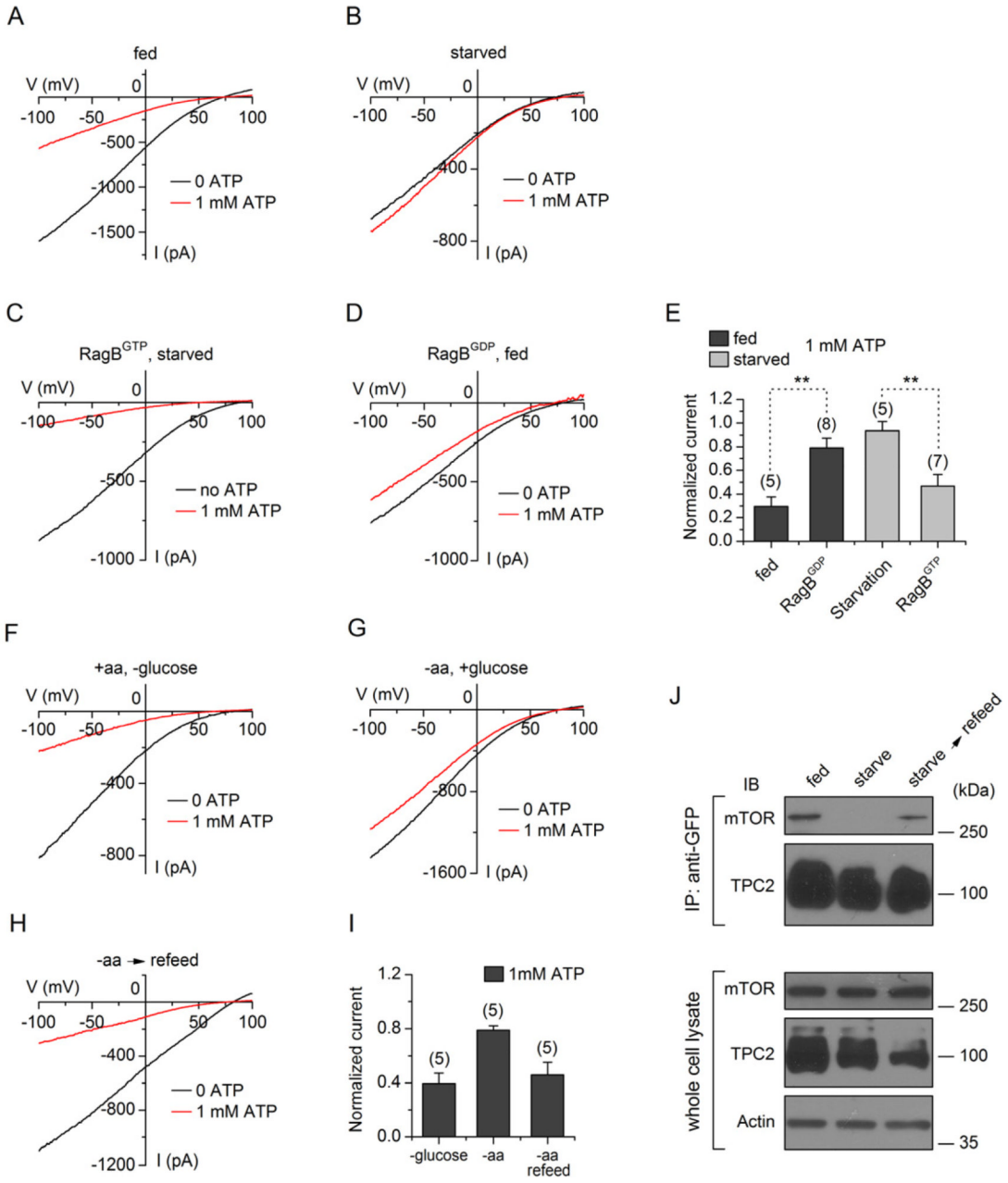

Figure 5. LysoNa$_{ATP}$ Detects Nutrient Deprivation

(A-E) Currents recorded from HEK293T cells transfected with TPC2 alone (A, B), or together with RagB^{GTP} (C) or RagB^{GDP} (D), were fed (A, D), or starved (B, C) in medium containing no glucose or amino acids for 60 min before recording. Current sizes normalized to those obtained without ATP (at −100 mV) are summarized in (E). ** indicates statistical significance ($p < 0.01$). (F-I) lysoNa$_{ATP}$ currents recorded from TPC2-transfected cells with treatments of glucose removal (F), amino acid removal (G) and amino acid re-fed (10 min) after removal (H). (J) Immunoblotting (IB) with whole cell lysates (lower 3 panels) or immunoprecipitates (IP with anti-GFP; upper 2 panels) from cells co-transfected with mTOR and GFP-tagged TPC2 with no treatment (control, fed), starvation (amino acid deprivation for 3h) or amino acid re-feeding after starvation (10x amino acid stimulation for

10 min). A weak mTOR band in the “starved” lane in the upper panel was visible after longer exposure (not shown). Data are presented as mean ± SEM.

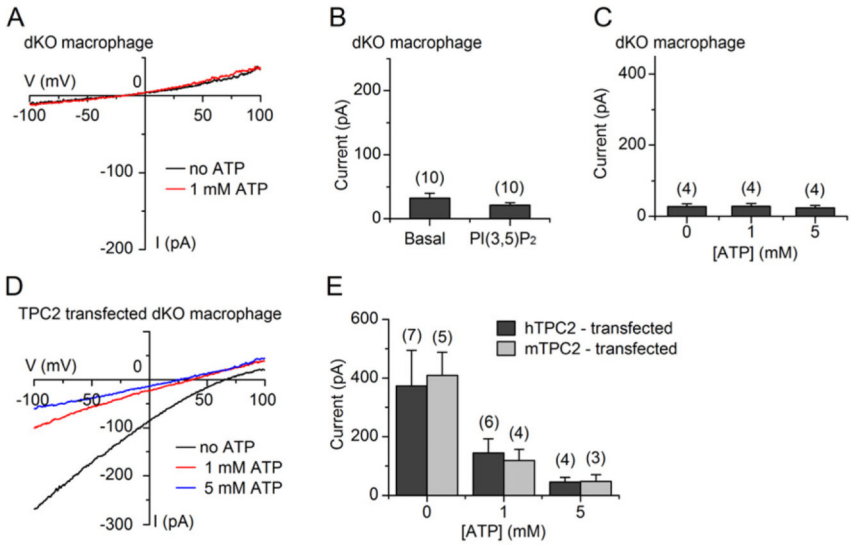

Figure 6. ATP-sensitive Current Is Absent in Endolysosomes of *tpc1*/*tpc2* Knockout Peritoneal Macrophages

Currents were recorded before the addition of $PI(3,5)P_2$ (basal), after 1 μM $PI(3,5)P_2$, and after application of ATP, from *tpc1*/*tpc2* dKO peritoneal macrophages. 1 μM $PI(3,5)P_2$ elicited no inward current (dKO: 32.1 ± 7.4 pA before $PI(3,5)P_2$, 20.9 ± 3.9 pA after $PI(3,5)P_2$, at −100 mV, n = 10; WT: 22.8 ± 5.8 pA before $PI(3,5)P_2$, 142.3 ± 3.5 pA after $PI(3,5)P_2$, n = 20). See also Figure 1C & D for comparison with WT. (D, E) Rescue of $lysoNa_{ATP}$ in the knockout macrophages with transfection of human (D, E) or mouse TPC2 (mTPC2) (E). Data are presented as mean ± SEM. See also Figure S4.

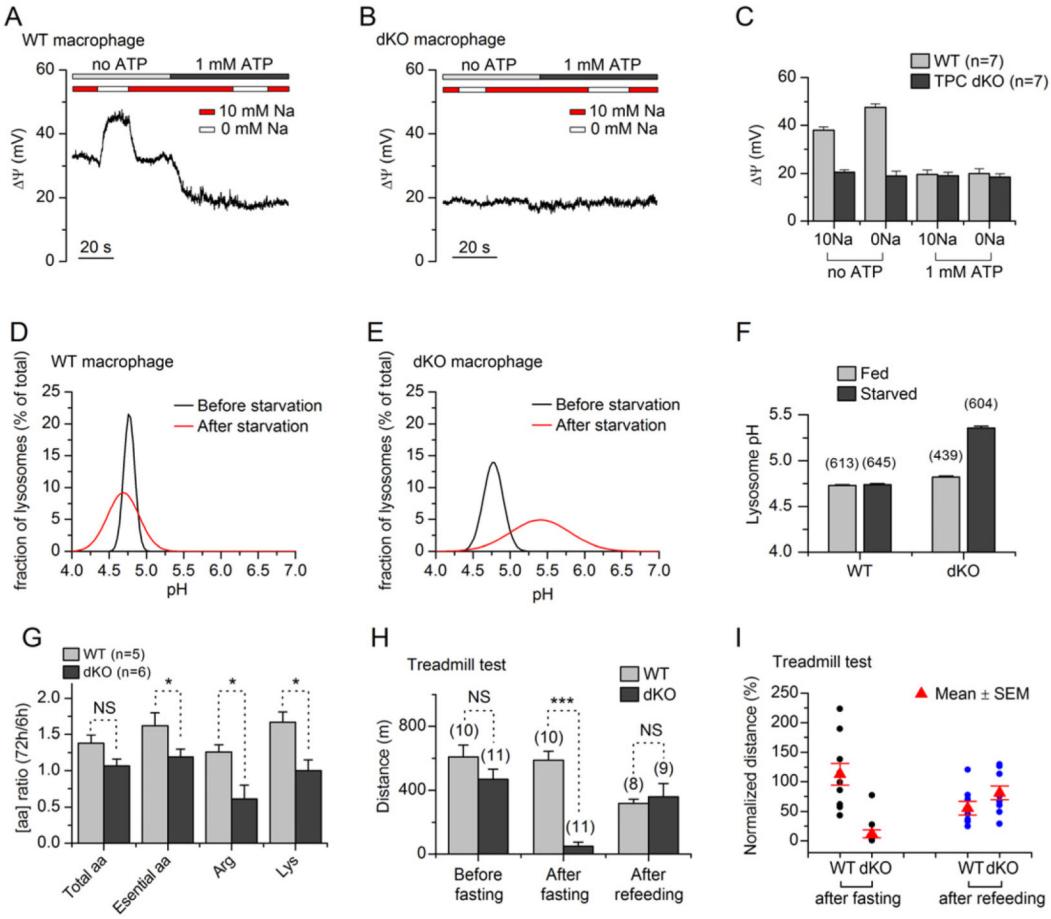

Figure 7. lysoNa$_{ATP}$s Control Lysosomal Membrane Potentials, Lysosomal pH, and Are Required for Normal Fasting Endurance

(A-C) Membrane potentials of macrophage lysosomes from wild-type (A) and dKO (B) were monitored with current clamp recordings while ATP was added to the bath containing 0 or 10 mM Na^+ as indicated by the bars above the recordings. (D-F) Lysosomal pH measured with ratio-metric imaging from WT (D, F) and dKO macrophage lysosomes (E, F) before and after starvation. Distribution histograms of pH values (fitted to Gaussian distributions) are in (D, E) and averaged values are in (*F*). (G) Amino acid analysis. Levels of 15 plasma amino acids (R, K, T, M, F, V, L, I, D, S, Q, G, A, Y, W) of each animal (5 to 6 in each group) were measured after 3 days of fasting and normalized to those at the beginning (6 hr) of fasting. (H, I) Mice were tested before and after fasting for 3 days, and 2 days after re-feeding. (H) Distance traveled at exhaustion. (I) Distance traveled of each mouse (represented by each point) after fasting and 2 days after re-feeding, as normalized to that before fasting. Black and blue circles indicate behavioral tests after fasting and after re-feeding conditions, respectively. Red triangles indicate mean values. Numbers of animals tested are in *(H)*. Several points overlap and are not distinguished. Asterisks indicate statistical significance (*, $p<0.05$; ***, $p< 0.001$). *NS*, not significant. Data are presented as mean ± SEM. See also Figure S5.